Arabian Journal of Geosciences (2018) 11: 146
https://doi.org/10.1007/s12517-018-3490-x

ORIGINAL PAPER

Mineralogy, Fluid inclusions and stable isotopes study constraints on genesis of sulfide ore mineral, Qaladiza area Qandil Series, Iraqi Kurdistan Region

Tola A. Mirza[1] · Saman Gh. Rashid[2]

Received: 23 December 2017 / Accepted: 15 March 2018 / Published online: 2 April 2018
© Saudi Society for Geosciences 2018

Abstract
The metalized quartz veins is located 5 km west of the Iraqi-Iran border in the Qandil range. The quartz veins included sulfide and oxide ore minerals which mostly occur in the form of open-space filling texture. The polymetallic mesothermal quartz veins are hosted by marble and phyllite rocks. Within these veins, multiphase, open-space filling and crustiform, bedding to massive textures with pyrite, sphalerite, galena, chalcopyrite,galena, sphalerite, tenorite, azurite, and malachite are observed. Selected samples were analyzed by using ore microscopy and electron probe micro analyzer (EPMA) and scanning electron microscope (SEM). Ore minerals show replacement textures. The paragenesis diagram was made from a careful study of polished sections and three stages have been identified including pre-stage mineralization, mineralization, and post-mineralization stages.

Fluid inclusion microthermometric analysis of 15 primary inclusions of quartz veins indicated that ore mineralization at the studied area were formed by a mesothermal, low to medium density, and dilute NaCl-type fluid system. The source of the fluid is mostly metamorphic which became mixed with other fluids later. Hydrothermal fluids of the selected studied area were classified into two groups based on microthermometry study; the first group had a higher homogenization temperature (335.5 to 386.8 °C) than the second group (194.1 to 298.5 °C), with a small difference in salinity between them. Nearly each group has different complexes including chloride and sulfide complexes respectively. The results of stable sulfur isotope of the ore minerals (chalcopyrite and sphalerite) confirmed the sedimentary and/or metamorphic origin of the ore mineralization.

Keywords Metallized quartz veins · Mesothermal · Hydrothermal fluids · Stable isotope

Introduction

The modern science of fluid inclusion geochemistry grew principally out of a new work on hydrothermal ore deposits more than 40 years ago (Roedder 1958). Mineral deposits are extraordinary anomalies in the Earth that provide us with perhaps the clearest evidence for the past flow of solutions through faults, fractures, and porous rocks that, in the process, dissolved, transported, and concentrated elements of economic interest. Looking at fluid inclusions trapped within hydrothermal veins was recognized as a direct way of saying much more than had previously been possible about the physicochemical condition during mineralization and the processes by which mineral deposits were formed (Wilkinson 2001). In this, nature was kind by providing an ideal sample material for investigation: often coarse-grained, transparent minerals with large fluid inclusions perfectly suited to the fledgling techniques of microthermometry and bulk chemical analysis.

Sulfur existing in approximately all natural environments may be a major constituent in ore deposits. These occurrences cover the whole temperature range of geological interest. Thus, it is quite clear that sulfur is of special interest in stable isotope geochemistry (Hoefs 2009). Therefore, the stable isotopic study of sulfur is another tool used as a key to defining ore genesis, especially for the ores that contained sulfur as a major element.

The sulphide mineralization is located in NE Iraq, close to the Iranian borders about 30 km from QaladizaTown (Fig. 1). It is one of the low-grade base metal sulphide Cu-Zn-Pb and

✉ Tola A. Mirza
tola.merza@univsul.edu.iq

[1] College of Science, Geology Department, University of Sulaimani, Sulaymaniyah, Iraq

[2] Geological Survey and Mineral Investigation of Sulaimani, Sulaymaniyah, Iraq

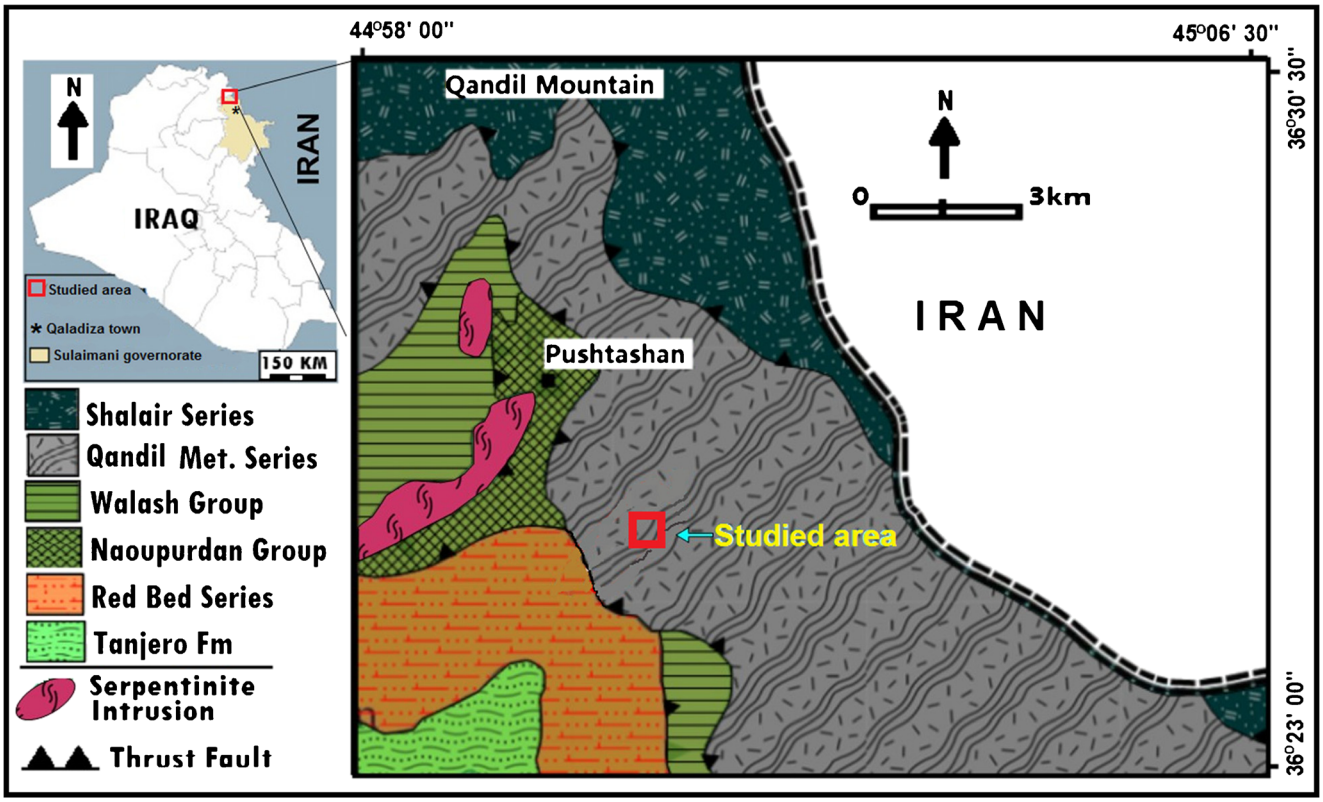

Fig. 1 Geological map of the studied area after Sissakian (1997)

Fe mineralization hosted by metacarbonate and phyllite of Qandil Series; it is well developed in shear zones and belongs to the northwestern part of the Zagros Orogen.

The Zagros belt resulted from the Late Cretaceous and Cenozoic convergence of the Iranian terranes and the Arabian Plate, when the intervening Neo-Tethys Ocean went through a succession of subduction, obduction, and collision stages (Alavi 1994; Sharland et al. 2001; Agard et al. 2005; Al-Qayim et al. 2012; Ismail et al. 2016).

The area was involved in the Cretaceous-Tertiary continental collision between the Afro-Arabian continent and the Iranian microcontinent (Alavi 1994, 2004; Mohajjel and Fergusson, 2000; Ghasemi and Talbot, 2006; Aliyari et al. 2009). Sulfide mineralization is associated with quartz veins that formed during regional deformation across the shear zones in metamorphic rocks of predominantly meta-meta carbonate and phyllite.

This paper presents a new mineral chemistry data, fluid inclusion and sulfur isotope study, which were collected from the two types of quartz veins in studied area, metalloid and non-metalloid quartz veins. New data in this study are used to determine the origin of ore-forming fluids and to infer the ore-forming fluid evolution. The results presented in this paper have implications for the genetic models of the metalloid quartz vein systems in the Qaladiza area and may be a useful guide for the exploration of similar sulfide mineralization provinces.

Geological setting

The metalized quartz veins is located 5 km west of the Iraqi-Iran border in the Qandil range locality of about 30 km north-northwest of Qaladiza town**.** The studied area represents a part of Qandil metamorphic series inside Penjween-Walash Zone (Fig. 1). Bolton (1958 in Buday 1980) used the term Qandil metamorphic series for a group of mostly low metamorphosed limestone and schist building the frontier ranges of eastern Iraq and structurally overlaying Walash and Naopurdan. According to Jassim and Goff (2006), regional metamorphism happened during the Late Cretaceous resulting in the deformation and metamorphism of the Qandil metamorphic series; however, the original textures of the rocks and their initial chemical properties have mostly been preserved, and they subdivided these series into three units from the youngest to the oldest as the (i) Mawat Group, (ii) Gimo Group, and (iii) Sirginil Group.

Dependent on the field investigation, the study area is a part of the Sirginil phyllite group. This group described by Buday (1980) is from the northern parts of the Bulfat massif (east of Qaladiza Town) up to the Rawanduz River valley in the NW in continuous outcrops, to the Penjween area in the SE, in the north of the Rawanduz River; only disconnected outcrops occur on the Hasar i Rust Mountain and along the Iranian border. Lithology of this group consists mostly of metamorphosed limestone, calcphyllites, and phyllites, sometimes

conglomerates without a more significant volcanic admixture. The unit was designated as the Sirginil sequence in accordance with the original name given by Bolton (1955). The age of Gimo and Sirginil sequences is supposed to be pre-Tertiary (Buday, 1980).

The studied area consists of alternation between medium beds of phyllite and massive beds of marble. They are cropped out as disconnected beds, sometimes brecciated and usually fractured with widespread of quartz veins and veinlets that cut across both phyllite and marble. The beds have a general dip of about 30°–40° N-NE. There are alternating beds of black and gray sheared limestone suffering from deformation, faulting, fracturing, folding, and thrusting; thus, the degree of weathering of the rocks is slightly high. All of the rock bodies have been thrusted over red bed series in the area (Fig. 1).

The quartz veins are structureless, homogeneous, and sometimes banded, with differences in size. Two types of quartz veins and veinlets have been identified in the studied area based on the ore mineral occurrences. The first one is metallized quartz vein and veinlets (MQV) which are related to ore minerals like chalcopyrite, galena, pyrite, hematite, malachite, and azurite. The second type is non-metallized quartz vein and veinlets (N-MQV) without any indication of metallic mineralization.

The sulfide ore mineralization mostly scattered irregularly inside metallized quartz veins or sometimes inside parent rocks and covered by gossan-type deposits. Most of the veins are associated with marble rocks. Sometimes, dendritic manganese oxidations are also noted especially on the marble rock beds. This manganese oxidation mostly occurs in fractures, bedding planes, and joint planes that make them pervious to water flow.

Sampling and analytical methods

Twelve selected samples were collected to prepare thin and polished sections to identify the ore minerals and their textures and ore mineral assemblages under plane- and cross-polarized light microscopes and reflected light microscope at the Department of Geology, Sulaimani University.

Twelve polished sections were used to identify the mineral chemistry by using an electron probe micro analyzer (EPMA) and scanning electron microscope (SEM) at the laboratory of the Institute of Mineralogy and Geology, University of Miskolc, Hungary, using JEOL JXA-8600 SUPERPROBE. Raw data were corrected with the ZAF correction program of Pouchou and Pichoir (1991). The applied accelerating voltage was 20 kV, and specimen current was 20 nA. Detection limits were 0.001 wt.%.

The fluid inclusion section was prepared from quartz-dominated sample. Microthermometric studies were carried out at the Dokuz Eylul University Geological Engineering Department–Fluid Inclusion Laboratory using a Linkam THMS600 freezing-heating stage mounted on a Leica DM LP microscope. Freezing-heating stage has ± 0.1 °C precision and temperature range varies from − 196 to 600 °C. The inclusions were monitored by the Hamamatsu C11440/ORCA-Flash 4.0 model infrared camera during the freezing-heating stage.

Two samples of sulfide ore minerals have been selected for sulfur isotope study at the laboratory of Queen's Facility for Isotope Research, Kingston, Ontario, Canada. Sulfide minerals (chalcopyrite and galena) have been separated from gangue minerals. Samples were weighed into tin capsules (4 × 6 mm) and the sulfur isotopic composition measured using a MAT 253 Stable Isotope Ratio Mass Spectrometer coupled to a Costech ECS 4010 Elemental Analyzer. The $\delta^{34}S$ values were calculated by normalizing the $^{34}S/^{32}S$ ratios in the sample to that in the Vienna Canyon Diablo Troilite (VCDT) international standard, values are reported using the delta (δ) notation in units of permil (‰) and are reproducible to 0.2‰.

Quartz vein occurrence

The ore zone of the studied area is manifested by generally various quartz vein types and veinlets. Two main types of quartz vein have been observed noted as metalloid and non- metalloid quartz vein. Generally, most of the quartz veins cut through the metamorphic carbonate rocks. The metalloid-bearing quartz accompanied with chalcopyrite, galena, sphalerite, and pyrite minerals (Fig. 2a). The non-metalloid quartz veins are without any indication of ore mineralization (Fig. 2b).

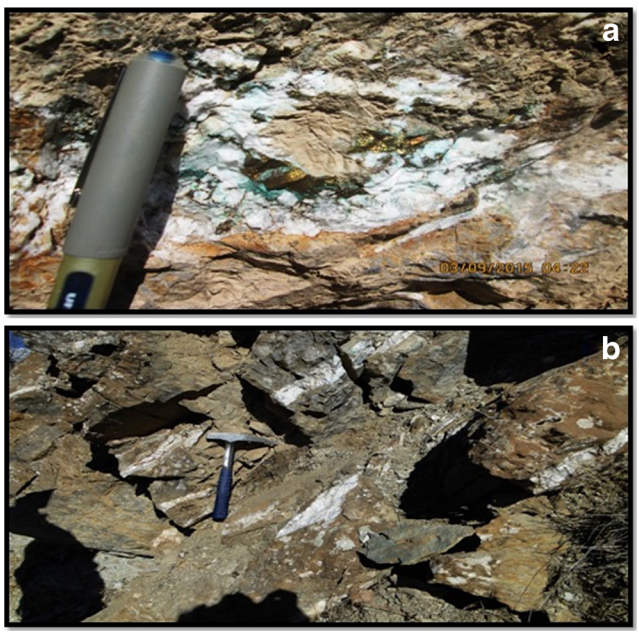

Fig. 2 **a** Sulfide ore mineralization inside metalized quartz veins (MQV). **b** Non-metalized quartz veins

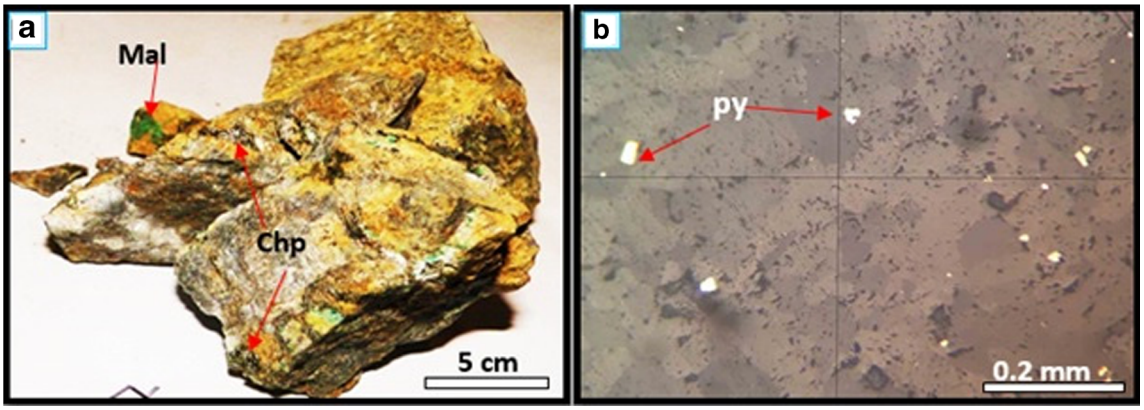

Fig. 3 **a** Marble shows disseminated chalcopyrite (cp) and malachite (mal) crustification. **b** Photomicrograph shows disseminated pyrite grains in marble

Mineralization style and hydrothermal alteration

Mineralization at the studied area is controlled by a combination of structural, alteration, and deformation factors. Local studies show that veins and their sulfide-bearing assemblage are associated with and deformed by a major phase of NW-SE shear zone, which corresponds with regional deformation (Jassim and Goff 2006). The ore mineralization of the studied area is controlled by a NW-SE trending, moderate to steeply dipping (NE) mylonitic shear zone, and dextral fault zone and is hosted by metacarbonate and phyllite rocks.

The sulfide mineralization and hydrothermal alteration occurs at least in two different styles. (1) The richest mineralization is associated with quartz-sulfide veins (Fig. 2a) that crosscut various lithological units and occurred parallel to ductile to brittle shear zone systems. Chalcopyrite is the dominant opaque mineral and is the major phase associated with sphalerite and galena.

(2) The second style of mineralization is characterized by an abundance of disseminated sulfide ore minerals in metamorphic rocks (marble and phyllite) (Fig. 3a, b).

Hydrothermal alteration, including chloritization, silicification, sulfidation, and most commonly dolomitization, are widely developed in the NW-trending shear zones and faults and its intensity progressively increases towards the sulfide ore bodies. The alteration mineralogy, replacement textures, and destruction of metamorphic minerals indicate a low to medium temperature metamorphic assemblage. The permeability and chemistry of the host rock controlled intensity and pattern of ore mineral scattering around veins (Cairns et al. 2001). The solution altered and replaced carbonates and precipitate sulfide ore minerals as open-space filling texture in carbonates (Fig. 4). Dolomitization and permeable facies in the carbonate host rocks could make suitable conditions for hydrothermal fluid migration and interaction with the host rocks. Oppositely, the absence of dolomitization and low-permeability facies precluded movement of hydrothermal fluids in the carbonate host rocks (Bazargani-Guilani et al. 2013).

Ore mineralogy and mineralization style

The study area consists of slightly metamorphosed rocks especially marble and some phyllite beds as host rocks.

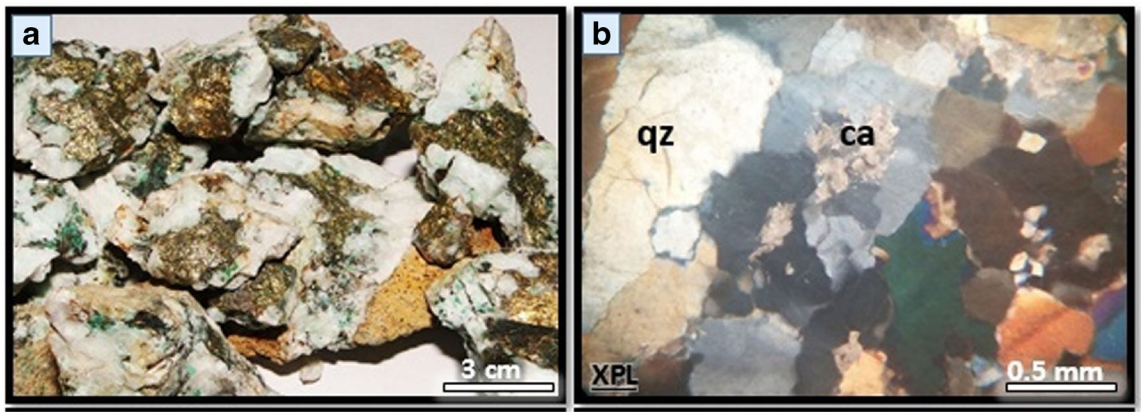

Fig. 4 **a** Photo of Quartz hosted sulfides and oxides ore minerals (MQV). **b** Photomicrograph of unhedral to subhedral quartz in which calcite is filling vugs

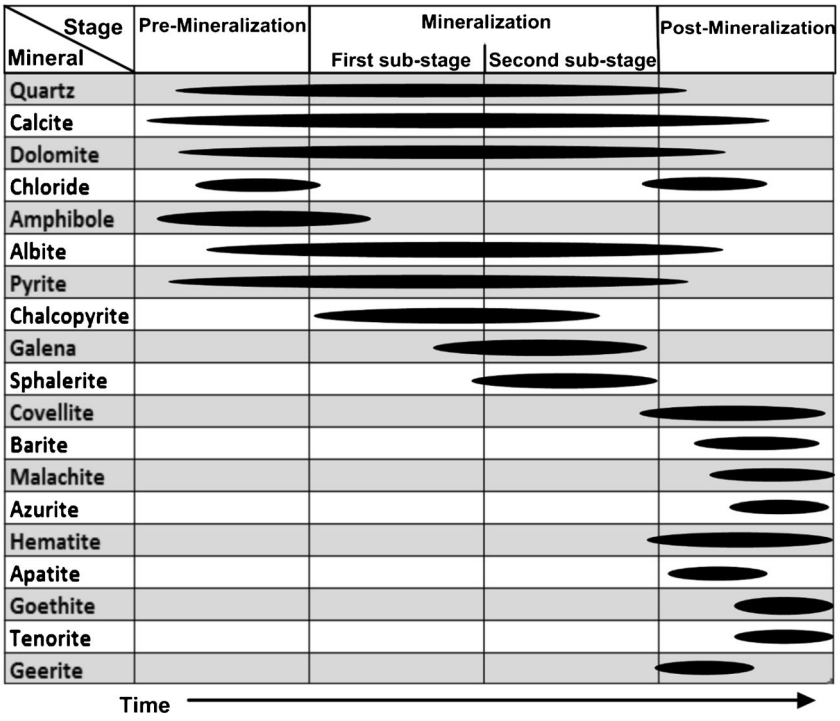

Fig. 5 Paragenetic diagram of ore-gangue minerals assemblage of polymetallic mesothermal quartz veins at the Sharosh area

Table 1 Trace element concentrations in minerals making up different types of ore at the Sharosh area

Mineral/element	(Wt%)						Atom per formula				
	Cu	Zn	Pb	Fe	S	Total	Cu	Zn	Pb	Fe	S
Chalcopyrite ($CuFeS_2$)											
Sp1	32.92	–		29.76	37.32	100.00	0.52	–		0.53	1.16
Sp2	33.13	–		29.67	37.20	100.00	0.52	–		0.53	1.16
Sp3	33.06	0.44		29.66	36.84	100.00	0.52	0.01		0.53	1.15
Sphalerite (ZnS)											
Sp 1	–	61.22		2.71	36.07	100.00	–	0.94		0.94	1.13
Sp2	–	61.75		2.41	35.84	100.00	–	0.94		0.94	1.12
Galena (PbS)											
Sp1			93.02		6.98	100.00			0.45		0.22
Sp2			94.01		5.99	100.00			0.45		0.19
Pyrite (FeS_2)											
Sp1	0.09	0.08		45.19	54.41	99.77				0.81	1.70
Sp2	0.24	0.20		45.64	53.37	99.45				0.82	1.66
Geerite ($Cu_{1.6}S$)											
Sp1	74.13			3.73	22.14	100.00	1.68			0.10	1.00
Sp2	74.11			3.61	22.25	99.97	1.68			0.06	1.00
Tenorite (CuO)	CuO	ZnO					CuO	ZnO			
Sp1	100.00	–				100.00	1.26	0.00			
Sp2	93.51	6.49				100.00	1.18	0.07			
Barite ($BaSO_4$)	SO_3	BaO					SO_3	BaO			
Sp1	35.58	64.42				100.00	0.44	0.42			
Sp2	34.78	65.12				99.90	0.43	0.42			

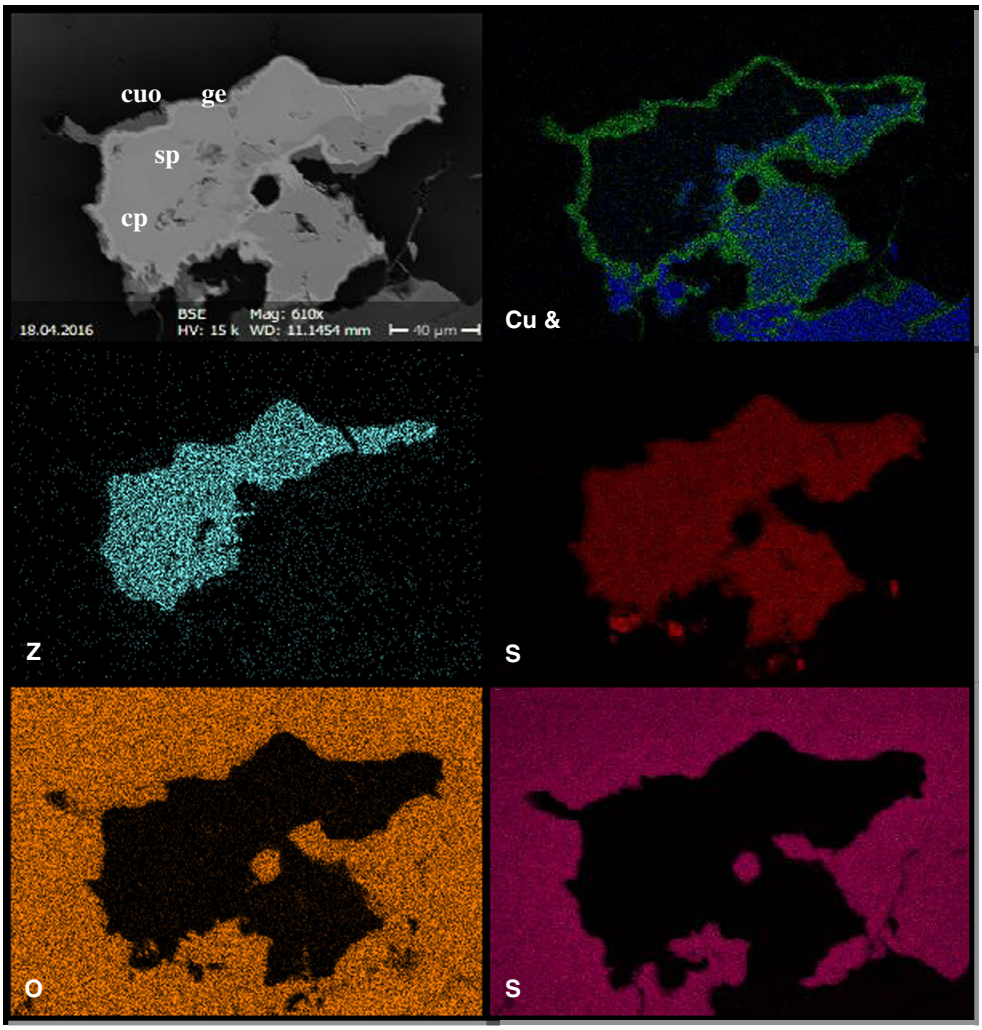

Fig. 6 BSE of mineralization zoning of sphalerite (sp) replaced by chalcopyrite (cp), gerrite (ge), and copper oxide (cuo) in quartz matrix, and shows elemental mapping of the different minerals

Different sizes of quartz veins, veinlets, and lenses are hosts of the ore mineralization, all of them representing the Qandil metamorphic rock unit. The most mineral constituents of outcropped rocks in the studied area are calcite, dolomite, quartz, and opaque minerals such as sulfides and oxides.

Macroscopically, the mineralized zones are grayish-black to green in appearance and seem to represent tectonically produced dilatant features filled with vein-type sulfide ores (Fig.4a) and it ranges in width from 1 cm to 3 m.

Compositionally, the quartz-sulfide-bearing ore consists mainly of medium-to-coarse-grained quartz and weakly strained anhedral to subhedral sulfide ore-coated quartz grains (Fig. 4b). In places, the grains exhibit extension, deformation, and recrystallization, implying ductile deformation. Sulfides form individual fine to medium grains occupying interstitial positions between the quartz grains and includes pyrite, chalcopyrite, galena, sphalerite, hematite, and goethite representing in total between 20 and 15% of the vein constituents.

Ore microscopy combined with the microprobe data and backscattered electron image revealed pre-mineralization (stage I) carbonate, silicate, and opaque minerals in the wall, including calcite, dolomite, plagioclase, chlorite, amphibole, quartz, muscovite, pyrite, and at least three assemblages of sulfide minerals in mineralized quartz veins and wall rock, which are interpreted as the mineralization stage (first sub-stage). The mineralization stage includes pyrite,chalcopyrite, sphalerite, galena crystals, and euhedral quartz; calcite-dolomite minerals are common mineral assemblages in the metalloid quartz veins (Fig. 5).

The later generation (second sub-stage) is dominated by chalcopyrite, pyrite, sphalerite, and galena. This assemblage occurs commonly in the metalloid quartz-sulfide veins as disseminations or accompanied with quartz, albite calcite gangue minerals (Fig. 5). Hematite, goethite, covellite, malachite, azurite, geerite, tenorite, barite, and apatite minerals are disseminated in the altered wall rocks as post-mineralization stage.

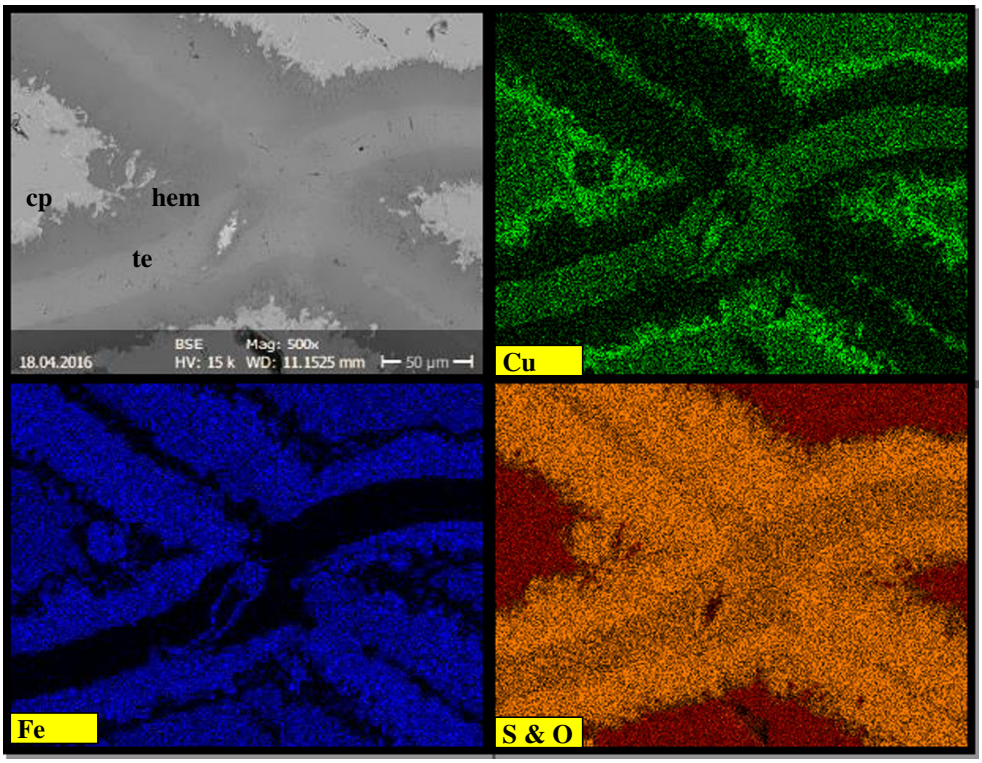

Fig. 7 Backscattered image (BSE) and elemental mapping illustrations chalcopyrite (cp), hematite (hem), and tenorite (te) minerals. Green color acts as copper (Cu), blue color acts as iron (Fe), red color acts as sulfur (S) and orange color as oxygen (O)

Ore minerals assemblages and their minerals chemistry

Chalcopyrite Microprobe analysis indicate the Cu, Fe, and S contents in chalcopyrite are ranging from Cu 33.49 ± 0.43%, Fe 29.71 ± 0.05%, and S 36.52 ± 0.32%, which shows typical chalcopyrite. Zn concentration in chalcopyrite is only 0.44% wt% (Table 1). This value can be considered being in a solid solution within the chalcopyrite lattice. Similar concentrations around 1 wt% was

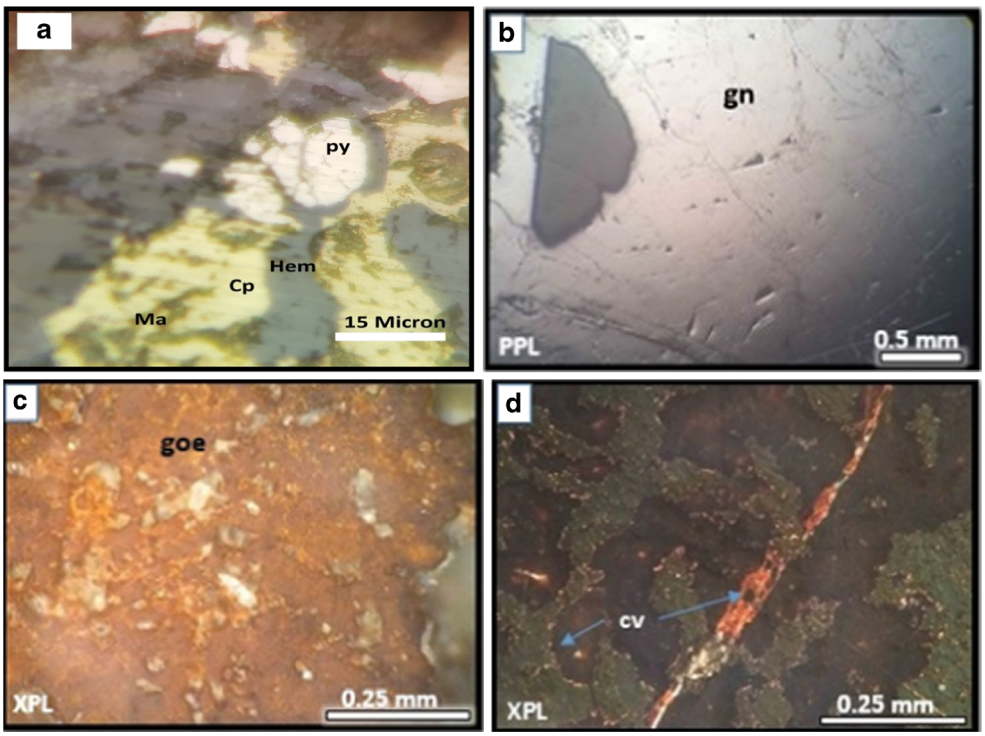

Fig. 8 **a** Brecciate texture of pyrite and replacement of pyrite (py) by hematite (Hem). **b** Deformed galena (gn) showing bands and characteristic triangular pits. **c** Goethite shows red brown internal reflection. **d** Covellite (cv) showing red to orange color, rim-replacement texture around chalcopyrite (cp), and vein filling texture

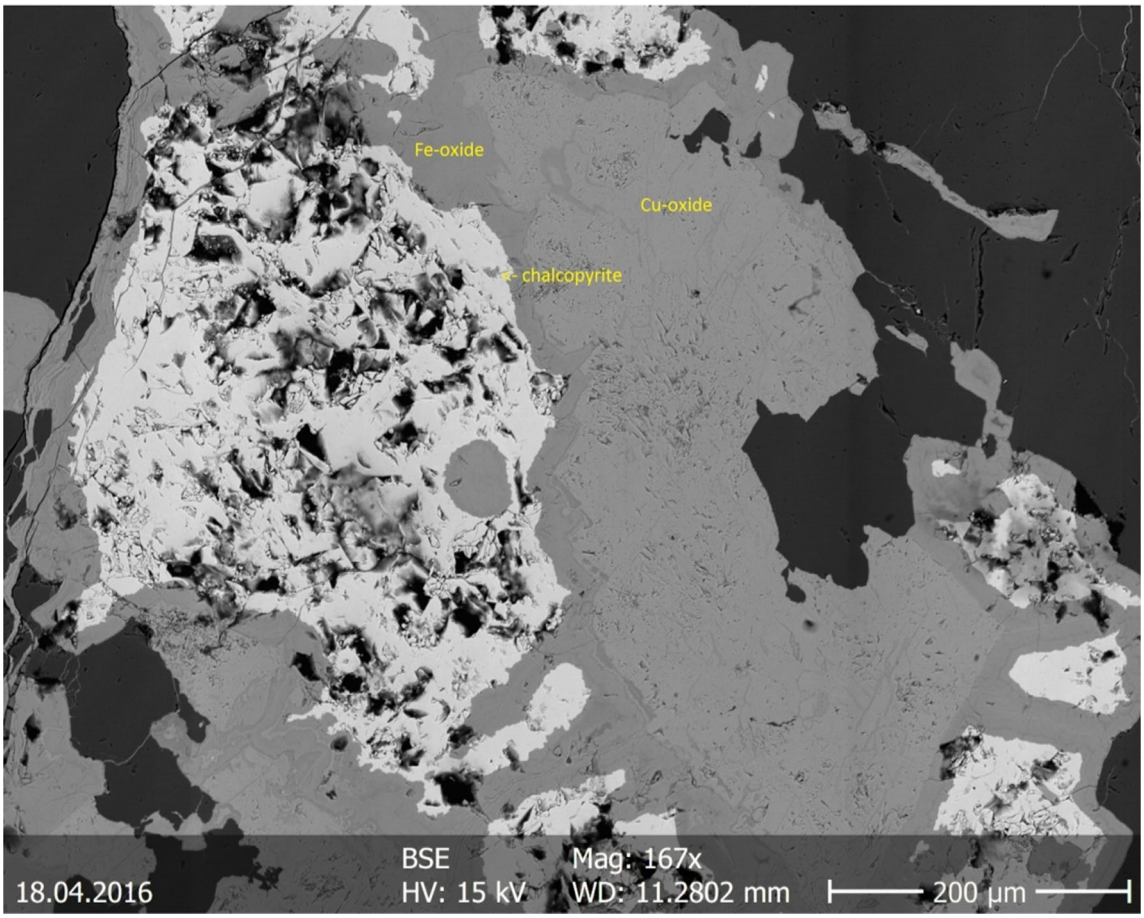

Fig. 9 Backscattered image (BSE) of copper oxide in studied samples

reported from experiments between 400 and 500 °C in the chalcopyrite stability field (Lusk and Calder 2004).

There is a limited substitution of Zn with Cu notwithstanding chalcopyrite having the similar crystal structure as sphalerite. The elemental mapping obviously shows iron oxides (hematite) and copper oxide (tenorite) replacement chalcopyrite (Figs. 6 and 7).

Pyrite Pyrite occurs in both host rock samples and vein samples. Some are replaced by Fe oxide minerals such as hematite. The pyrite shows weak anisotropy abnormality and brecciated texture which indicates that the rocks were subjected to stress (Fig. 8a). This phenomenon is the most typical texture developed under low-grade metamorphic conditions (McClay and Ellis 1983; Lianxing and McClay 1992). The average contents (wt.%) of Fe and S in pyrite are 45.42 and 53.89 wt% respectively and show a typical chemical formula of pyrite Fe S_2 (Table 1).

Galena Galena is another common ore mineral in this research. Some of galena shows a typical texture of triangular pits (Fig. 8b). The Pb concentrations of galena measured by electron microprobe in analyzed two spots shows that the Pb content ranges between 93.02 and 94.01 wt.%, and low sulfur content ranges from 6.98 to 5.99 wt% (Table 1). Typical Pb and S contents in galena are 86 and 7 wt.% respectively. Kullerud (1969) described this composition as Pb-PbS. This extra Pb that is contained in this spot may be related to the contamination through polishing and grinding of the sample.

Sphalerite Sphalerite is an uncommon mineral in samples that are observed as very fine grains and replacement texture that are replaced by chalcopyrite and iron oxides (Figs. 6). It shows a simple chemical composition in the system (Zn, Fe, S). The composition of sphalerite is characterized by weak variations in its Fe contents. The Fe and Zn contents in sphalerite ranges from 2.41 to 2.71 wt.% and 61.22 to 61.75 wt.% respectively (Table 1). Iron is a solitary minor element in sphalerites which is a substitute for Zn. The sphalerite grain is replaced by chalcopyrite and iron oxide, while all of them are surrounded by quartz, and thus shows mineralization zoning (Fig. 6). Kalogeropoulos (1982) have convinced that this is evidence of chalcopyrite disease which is a cancerous replacement produced by Cu in aqueous solution reacting with FeS in sphalerite.

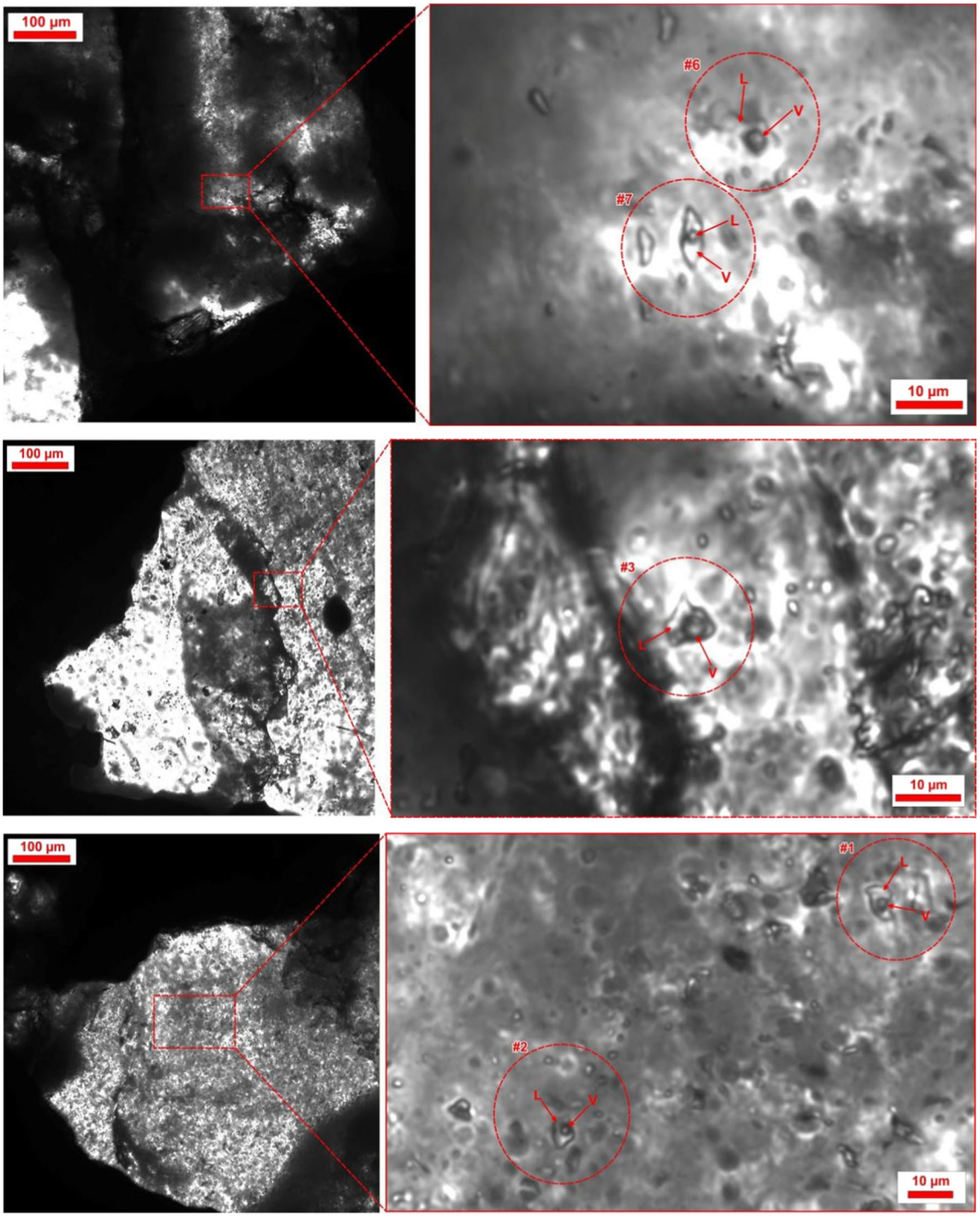

Fig. 10 Photomicrographs of the studied fluid inclusions

Tenorite Tenorite is a secondary copper oxide which occurs in the oxidized or weathered zone. The CuO content in tenorite ranges between 100 and 93.51 wt.% (Table 1) (Figs. 7 and 9). CuO commonly occurs with chrysocolla and the copper carbonates such as azurite and malachite (Ramdohr 2013).

Gerrite Gerrite is replacing sphalerite along cleavage traces and occurs as thin black plates (Fig. 6). The Cu content in the gerrite is (74.13 wt.%), while the S content is 22.14 wt.%. The gerrite shows a very limited content of iron 3.73 wt.% (Table 1).

Barite The barite composition shows that the BaO content is 64.42 wt.% and SO_3 35.58 wt. % (Table 1). Barite commonly occurs in Pb-Zn veins in limestones, in hot spring deposits, and with hematite ore (Hanor 2000).

Table 2 Microthermometric results and dimensions of fluid inclusions in SH-11V sample. (Each number (#) of measurement were given on microphotograps)

No. (#)	Tm_{ice}	Tm_{first}	Th	Salinity	Area (inclusion)	Area (bubble)	Length	Mineral	V/L
1	−2.2	−48	262.9	3.7	38.4	7.3	9.6	Quartz	0.19
2	−2.5	−45	239.5	4.2	27.8	5.8	8.8	Quartz	0.21
3	−1.9	−43	359.1	3.2	39.0	12.3	9.2	Quartz	0.32
4	−4.6	−38.6	265.5	7.3	35.3	6.4	9.5	Quartz	0.18
5	−2.6	−41	386.8	4.3	165.3	51.4	19.3	Quartz	0.31
6	−3.6	−35	244.7	5.9	49.3	10.7	12.9	Quartz	0.22
7	−3.1	n.a.	194.1	5.1	23.9	3.9	11.8	Quartz	0.16
8	−1.5	−40.5	315.9	2.6	49.5	10.4	12.5	Quartz	0.21
9	−3.2	−39	266.3	5.3	23.1	6.8	8.6	Quartz	0.29
10	−3.5	n.a.	298.5	5.7	14.1	4.6	7.3	Quartz	0.33
11	−3.5	−39	348.4	5.7	23.2	11.6	7.7	Quartz	0.50
12	−2.2	−39	335.5	3.7	54.2	12.3	15.9	Quartz	0.23
13	n.a	n.a.	267.8	n.a.	n.a.	n.a.	n.a.	Quartz	n.a.
14	−2.8	−41.6	286	4.6	16.7	5.6	7.2	Quartz	0.34
15	−3.2	−41	250.4	5.3	22.8	4.9	10.0	Quartz	0.21
Mean	−2.9	−40.9	288.1	4.8	41.6	11.0	10.7		0.26
Median	−3.0	−40.8	267.8	4.9	31.6	7.1	9.6		0.22

Goethite Goethite is also observed as a vein filling texture and as a secondary mineral formed by the oxidation of sulfides such as pyrite and chalcopyrite under surface weathering circumstances (Fig.8c).

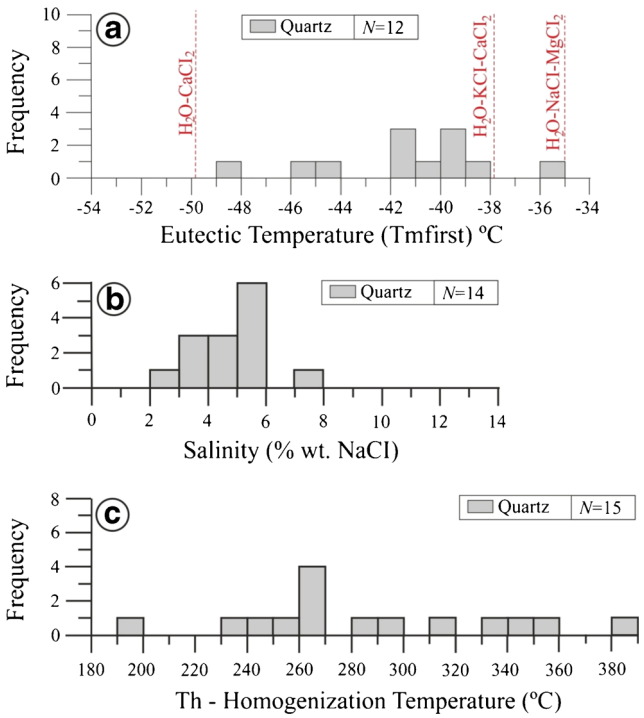

Fig. 11 Frequency distributions of eutectic, salinity, and homogenization temperatures of measured fluid inclusions from SH-11V sample

Azurite and malachite Azurite and malachite are found as hydrothermal alteration minerals. They are clearly observed on the surface of mineralization areas (Figs. 3a).

Covellite The replacement of chalcopyrite with covellite is also observed in weathered ores (Fig. 8d). This happens when iron is preferentially removed from chalcopyrite, forming bornite, and later chalcocite, covellite, and digenite (Kant et al. 2014).

Fluid inclusion study

The only liquid-rich inclusions were observed during fluid inclusion petrography studies. These are classified as primary and liquid-rich inclusions, which were commonly observed as isolated single inclusions in quartz crystals (Fig. 10). A total of 15 microthermometric measurements were performed on these primary liquid-rich inclusions. The microphotographs of these fluid inclusions (Fig.10) and the fluid inclusion microthermometric results are given in Table 2. Freezing-heating stages and fluid inclusion assemblages were selected based on the criteria and recommendations of Roedder (1958, 1984), and Goldstein (2003). Salinities (wt.% NaCl equivalents) were calculated from the last ice melting temperatures using equation of Bodnar (1993). The inclusions have a variation in size from 7.2 to 19.3 μm and a vapor/liquid/ (V/L) ratio range from 18 to 50%. Although the size of inclusions is mostly smaller than 10 μm, microthermometric measurements were successfully performed by using high-solution infrared camera.

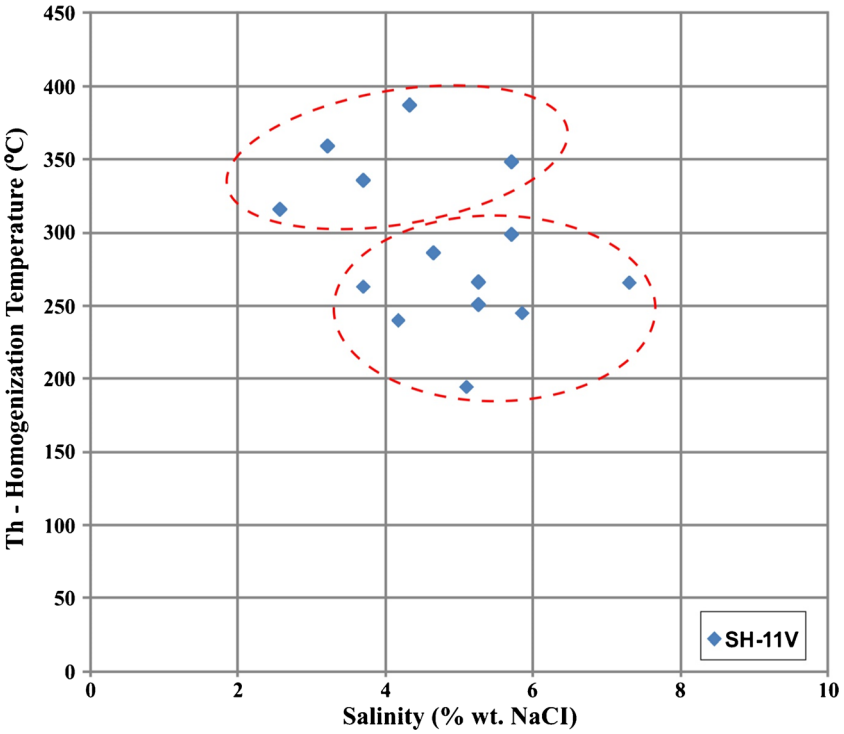

Fig. 12 Homogenization temperature vs salinity (wt.% NaCl equiv.) diagram of measured fluid inclusions from SH-11V sample

The first melting temperatures are in the interval between −35 and −48 °C, indicating H_2O-KCl-$CaCl_2$-NaCl are the principal components of the ore-forming fluids, possibly with smaller amounts of $MgCl_2$ (Fig. 11a). The ice melting temperatures from quartz vary from −1.5 to −4.6 °C, which correspond to a salinity range from 2.6 to 7.3 wt.% NaCl equivalents with an average of 4.8 wt.% NaCl equivalent (Fig. 11b). These inclusions yield homogenization temperatures from 194.1 to 386.8 °C with an average of 288.1 °C (Fig. 11c).

The results show two different inclusion groups which represent the homogenization temperature interval between 335.5 to 386.8 °C for the first group and 194.1 to 298.5 °C for the second group (Fig. 12). On the other hand, there are no substantial differences in terms of the salinity of these two groups ranging from 2.6 to 5.7 wt.% for the first group and 3.7 to 7.3 wt.% for the second group.

These differences in homogenization temperatures may be caused by cooling towards the outer zones of quartz. Therefore, the first group is considered to characterize the early stage of the mineralization due to the highest homogenization temperatures obtained from quartz (max 386.8 °C). Also, these differences may be caused by a mixing of two different ore-forming fluids.

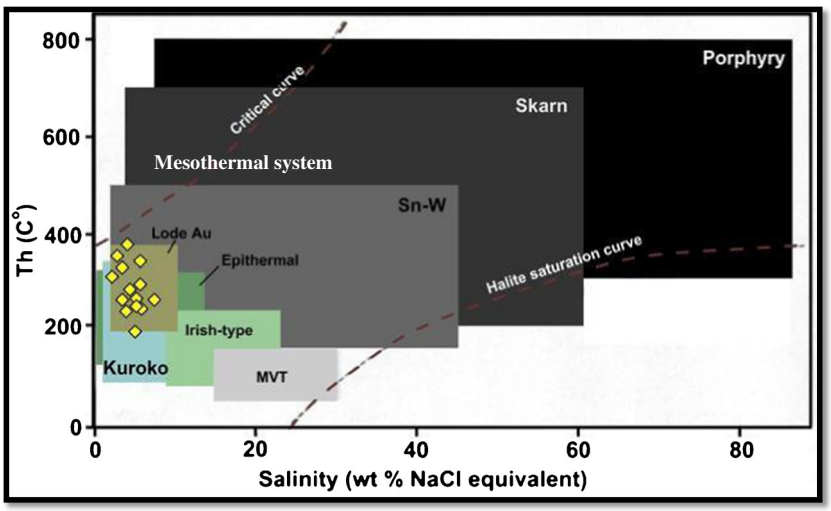

Fig. 13 Salinity-homogenization temperature diagram to determine ore mineralization type (after Wilkinson 2001)

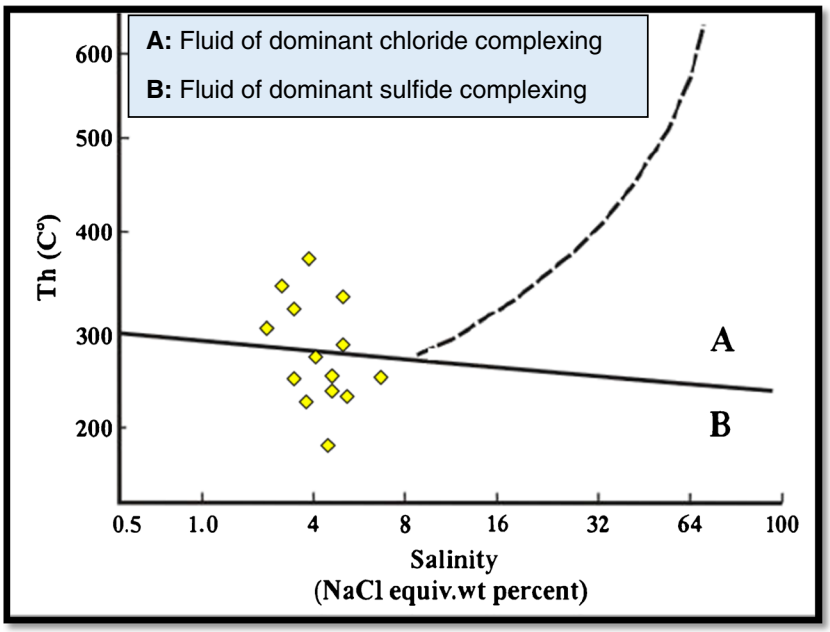

Fig. 14 Homogenization temperature-salinity diagram to determine Sharosh ore mineral complex (Pirajno, 2009) with location of studied samples

The microthermometry results show that these sulfide ore minerals has been formed in a medium temperature range and categorized as a mesothermal (informally called lode Au) mineral deposit type (Wilkinson 2001) (Fig. 13). The fluid salinity and homogenization temperatures indicate that both chloride and sulfide complexes could have a conspicuous role in the formation of this ore minerals (Pirajno 2009) (Fig. 14). Also, the homogenization temperature and salinity information show that the studied fluid inclusions are characteristic of a metamorphic fluid regime which became a mixture fluid later (Fig. 15). Most of the metamorphic fluids have low salinities, dominantly small size of secondary inclusions, and a low concentration of reduced sulfur (Roedder 1984); globally, fluids of this nature are implicated in the formation of orogenic gold deposits which represent a very important category of gold deposit types (Phillips et al. 1994, Daniel et al. 2017; Ralica et al. 2017). Nevertheless, it would be illogical to ignore the influence of meteoric waters in the formation of this ore minerals, while the existence of low salinity fluid inclusions (< 5% wt. eq. NaCl) point to that meteoric water

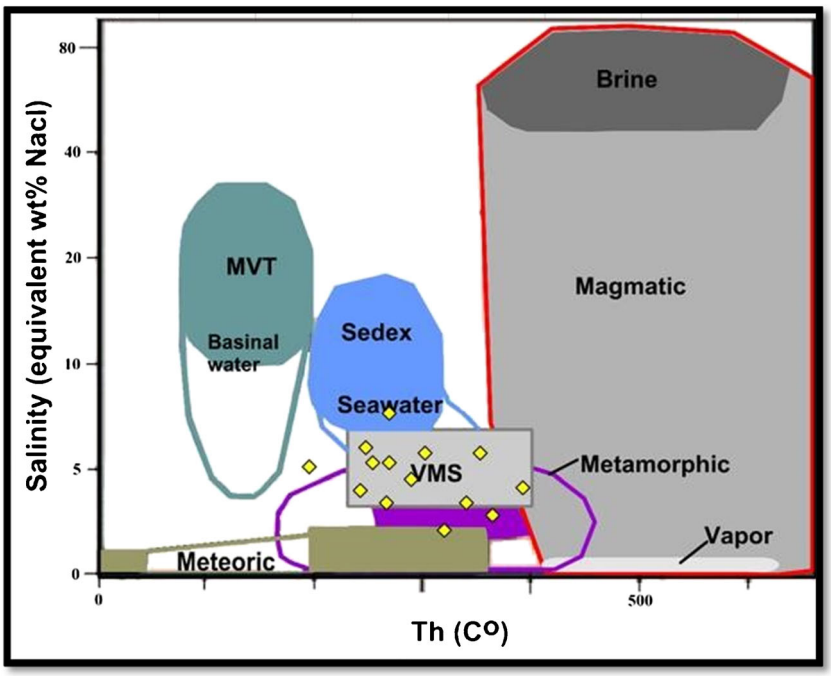

Fig. 15 Determination of the ore fluid type using a homogenization temperature salinity diagram (dark zones inside lines show approximate T-salinity range for ore-forming fluids) after Kesler (2005)

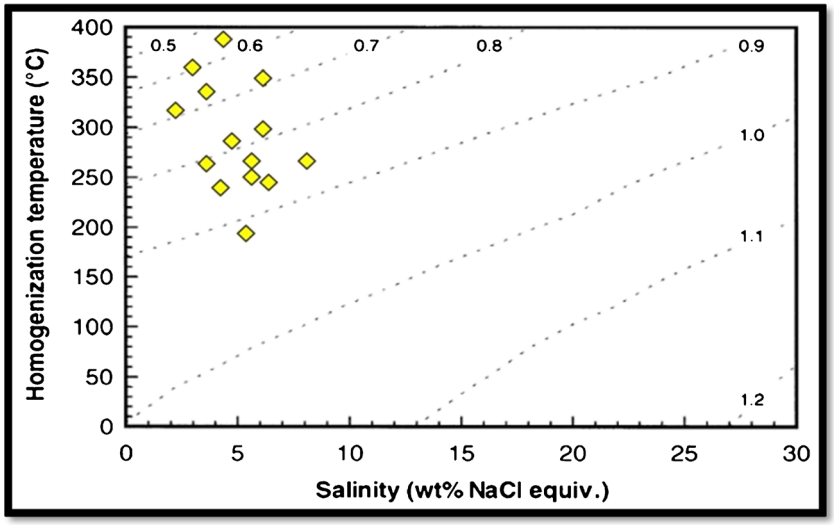

Fig. 16 Diagram of salinity-homogenization temperature to determine the density (Bodnar 1983) with location of studied samples

probably had a prominent role in the formation of the ore minerals (Kuhanestani et al. 2014).

Density of the fluid will be discover via conventional plotting between homogenization temperature and salinity results irrespective of fluid trapping conditions (Bodnar 1983) (Fig. 16). Inclusions of the studied samples exhibit a slightly wide range of density (ranges from more than 0.9 to less than 0.6 g/cm^3). Differences in fluid density are particularly significant with respect to mechanisms of fluid flow and evaluation of spatial variations in fluid density in a system can provide constraints on the flow process (Wilkinson 2001).

Sulfur isotopes

Sulfur, the 10th most abundant element in the universe and the 14th most abundant element in the Earth's crust, is the defining element of sulfide minerals and provides insights into the origins of these minerals through its stable isotopes. The insights come from variations in the isotopic composition of sulfide minerals and related compounds such as sulfate minerals or aqueous sulfur species, caused by preferential partitioning of isotopes among sulfur-bearing phases, known as fractionation. These variations arise from differences in temperature, or more importantly, oxidation and reduction reactions acting upon sulfur. The oxidation and reduction reactions can occur at high temperatures, such as in igneous systems, at intermediate temperatures, such as in hydrothermal systems and at low temperatures during sedimentary diagenesis (Seal 2006).

The $\delta^{34}S$ values of Sharosh chalcopyrite and galena occupy a narrow range − 17.7 and − 17.6‰ respectively with an average value of − 17.65‰. This range is very close compared with the values of $\delta^{34}S$ by Hoefs (2009); Seal (2006); Ohmoto

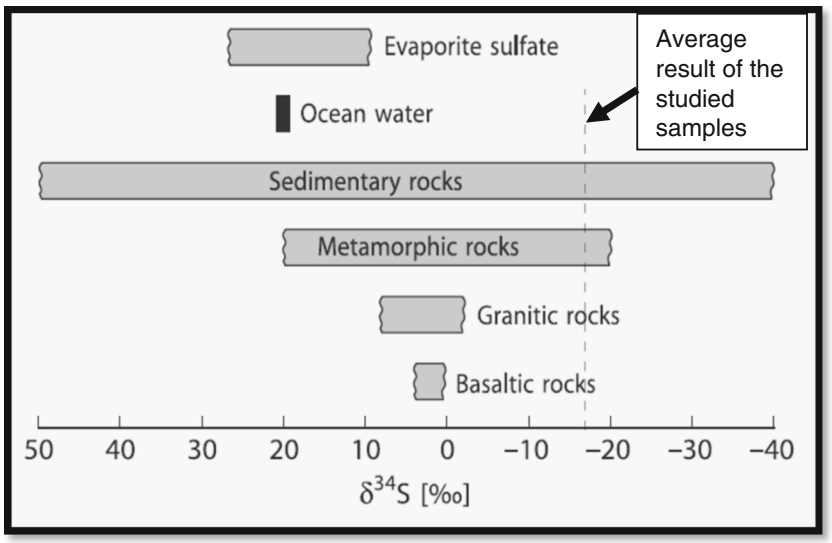

Fig. 17 Sulfur isotope composition of chalcopyrite and galena from the Sharosh area. Results signed by dashed line intersect with isotopic range of sedimentary and metamorphic sources (after Hoefs 2009)

(1986); Nielsen (1979); Ohmoto and Rye (1979) and appears that $\delta^{34}S$ values of studied sample plots in the range of values assigned to sedimentary and metamorphic sources of sulfur Sharosh (Fig. 17).

Conclusions

Common ore minerals of the polymetallic mesothermal quartz veins at thestudied area are chalcopyrite ($CuFeS_2$), galena (PbS), sphalerite (ZnS), pyrite (FeS_2), azurite, malachite, gerrite, tenorite covalite, hematite, and other Fe oxide minerals. Common textures of ore minerals are open-space filling textures and replacement textures. The paragenesis diagram was drawn from a study of polished sections under microscope. Ore mineral textures have been interpreted to identify the order of deposition and to make the paragenesis diagram. Quartz, calcite, dolomite, and pyrite are formed in early stage (pre mineralization) and pyrite, chalcopyrite, galena, and sphalerite represent a mineralization stage while geerite, covelite, tenorite, azurite, malachite, and Fe oxide minerals represent a post-mineralization order of deposition.

The microthermometry results show that these sulfide ore minerals have been formed in a low to medium density, dilute NaCl-type fluid system, and medium temperature range and categorized as a mesothermal. Two types of fluid inclusions are present in the studied samples. Type 1 have high homogenization temperature ranges between 335.5 to 386.8 °C; type 2 inclusions show lower homogenization temperature ranges between 194.1 to 298.5 °C. With no substantial differences in terms of salinity of these two groups ranging from 2.6 to 5.7 wt.% NaCl eq. for the first group and 3.7 to 7.3 wt.% NaCl eq. for the second group.

Stable isotopic compositions of $\delta^{34}S$ suggest that sulfur in the hydrothermal fluid were derived from the sedimentary and metamorphic country rocks.

Acknowledgments We are grateful to Professor Dr. Harald G. Dill, Federal Institute for Geosciences and Natural Resources/Hannover, for his insightful suggestions and comments. We are indebted to the three anonymous referees for their constructive and critical reviews, which greatly helped us to improve this paper. We are particularly grateful to the laboratory of the Institute of Mineralogy and Geology, University of Miskolc, Hungary, for doing EPMA and SEM analysis.

References

Agard PJ, Omrani L, Jolivet, Mouthereau F (2005) Convergence history across Zagros (Iran):Constraints from collisional and earlier deformation. Int J Earth Sci 94(3):401–419

Alavi M (1994) Tectonics of the Zagros orogenic belt of Iran: new data and interpretation. J Tectonophys 229(3):211–238

Alavi M (2004) Regional stratigraphy of the Zagros fold-thrust belt of Iran and its proforeland evolution. Am J Sci 304(1):1–20

Aliyari F, Rastad E, Mohajjel M, Arehart GB (2009) Geology and geochemistry of D–O–C isotope systematics of the Qolqoleh gold deposit, northwestern Iran: implications for ore genesis. Ore Geol Rev 36(4):306–314

Al-Qayim B, Omer A, Koyi H (2012) Tectonostratigraphic overview 566 of the Zagros 567 Suture Zone, Kurdistan Region, Northeast Iraq. GeoArabia 17:109–156

Bazargani-Guilani K, Rabiei M, Mehrabi B (2013) Effects of host rock mineralogical composition and sedimentary facies on development of geochemical halos in Shahmirzad Pb-Zn deposits, central Alborz, Iran. J Geochem Explor 124:155–165

Bodnar RJ (1983) A method of calculating fluid inclusion volumes based on vapor bubble diameters and PVTX properties of inclusion fluids. Econ Geol 78(3):535–542

Bodnar RJ (1993) Revised equation and table for determining the freezing point depression of H_2O-NaCl solutions. Geochim Cosmochim Acta 57(3):683–684

Bolton C M G (1955) Report on the geology and economic prospects of the Rowanduz area. Site Inv. Co. report. NIMCO Library. Baghdad

Buday T (1980) The regional geology of Iraq, stratigraphy and paleogeography, Dar AL-Kuttib Pub. House. University of Mosul, Iraq. 445p

Cairns CJ, McQueen KG, Leah PA (2001) Mineralogical controls on element dispersion in regolith over two mineralised shear zones near the Peak, Cobar, New South Wales. J Geochem Explor 72(1):1–21

Daniel M, Darcy B, Bodnar RJ (2017) Mineralogical, petrographic and fluid inclusion evidence for the link between boiling and epithermal Ag-Au mineralization in the La Luz area, Guanajuato Mining District, México. Ore Geol Rev 89:143–170

Ghasemi A, Talbot CJ (2006) A new tectonic scenario for the Sanandaj–Sirjan Zone (Iran). J Asian Earth Sci 26(6):683–693

Goldstein RH (2003) Chapter two: Petrographic analysis of fluid inclusions, In Fluid inclusions analysis and interpretation edited by I. Samson, A. Anderson, & D. Marshall, eds. Mineral. Assoc. Can., Short Course Ser. 32, 9–53

Hanor JS (2000) Barite–celestine geochemistry and environments of formation. Rev Mineral Geochem 40(1):193–275

Hoefs J (2009) Stable isotope geochemistry. Springer-Verlag, Berlin

Ismail S. A, Ali S A, Nutman A P, Bennett VC, Jones B G. (2016) The Pushtashan juvenile suprasubduction zone assemblage of Kurdistan (northeastern Iraq): a cretaceous (Cenomanian) Neo-Tethys missing link. Geosci Front

Jassim S.Z, Goff JC eds. (2006) Geology of Iraq, DOLIN, sro, distributed by Geological Society of London

Kalogeropoulos SI (1982) Chemical sediments inthe hanging wall of volcanogenic massive sulfide deposits. Ph.D. thesis, Univ. Toronto, 488 p

Kant W, Warmada IW, Idrus A, Setijadji LD, Watanabe K (2014) Ore mineralogy and mineral chemistry of pyrite, galena, and sphalerite at Soripesa prospect area, Sumbawa Island, Indonesia. J Appl Geol 4(1):1–14

Kesler SE (2005) Ore-forming fluids. Elements 1(1):13–18

Kuhanestani NM, Mohammadi BM, Alderton DHM, Tabatabaei SH, Bagheri H (2014) Mineralogical and geochemical studies on the Gowd-e-Morad (Ni, Co, As–Cu) mineral deposit Anarak (central Iran). Arab J Geosci 7(11):4779–4791

Kullerud G (1969) The lead-sulfur system. Am J Sci 267:233–256

Lianxing G, McClay KR (1992) Pyrite deformation in stratiform lead-zinc deposits of the Canadian Cordillera. Mineral Deposita 27(3):169–181

Lusk J, Calder BOE (2004) The composition of sphalerite and associated sulfides in reactions of the Cu-Fe-Zn-S, FeZn-S and Cu-Fe-S systems at 1 bar and temperatures between 250 and 535°C. Chem Geol 203:319–345

McClay KR, Ellis PG (1983) Deformation and recrystallization of pyrite. Mineral Mag 47(4):527–538

Mohajjel M, Fergusson CL (2000) Dextral transpression in Late Cretaceous continental collision, Sanandaj–Sirjan zone, western Iran. J Struct Geol 22(8):1125–1139

Nielsen H (1979) Sulfur isotopes. In: Jager E, Hunziker J (eds) Lectures in isotope geology. Springer, Berlin, pp 283–312

Ohmoto H (1986) Stable isotope geochemistry of ore deposits. Rev Mineral Geochem 16(1):491–559

Ohmoto H, Rye RO (1979) Isotopes of sulfur and carbon. In: Barnes HL (ed) Geochemistry of hydrothermal ore deposits, 2nd edn. John Wiley and Sons, New York, pp 509–567

Phillips GN, Williams PJ, De Jong G (1994) The nature of metamorphic fluids and significance for metal exploration. Geol Soc Lond, Spec Publ 78(1):55–68

Pirajno F (2009) Hydrothermal processes associated with meteorite impacts. In: Hydrothermal Processes and Mineral Systems. Springer, Dordrecht, pp 1097–1130

Pouchou JL, Pichoir F (1991) Quantitative analysis of homogeneous or stratified micro volumes applying the model "PAP". In: Electron probe quantitation, Springer US, pp. 31–75

Ralica S, Vassilka M, Aberra M (2017) Ore petrology, hydrothermal alteration, fluid inclusions, and sulfur stable isotopes of the Milin Kamak intermediate sulfidation epithermal Au-Ag deposit in Western Srednogorie, Bulgaria. Ore Geol Rev 88:400–415

Ramdohr P (2013) The ore minerals and their intergrowths. Elsevier

Roedder EW (1958) Technique for the extraction and partial chemical analysis of fluid-filled inclusions from minerals. Econ Geol 53(3): 235–269

Roedder E (1984) Fluid inclusions. Mineral Soc Am Rev Mineral 12:644

Seal RR II (2006) Sulfur isotope geochemistry of sulfide minerals. Rev Mineral Geochem 61:633–677

Sharland PRR, Archer DM, Casey RB, Davies SH, Hall AP, Heward AD, Horbury SMD (2001) Arabian Plate sequence stratigraphy, GeoArabia Special Publication 2, Gulf Petro Link, Bahrain, 371 p., with 3 charts

Sissakian VK (1997) Geological map of Arbeel and Mahabad Quadrangles Sheets, NJ 38-14 and NJ 8-15 Scale 1:250000. Geological survey and mining, Iraq

Wilkinson JJ (2001) Fluid inclusions in hydrothermal ore deposits. Lithos 55:229–272